NANO LETTERS

2007
Vol. 7, No. 9
2563−2567

Template-Grown NiFe/Cu/NiFe Nanowires for Spin Transfer Devices

Luc Piraux,*,† Krystel Renard,† Raphael Guillemet,‡ Stefan Mátéfi-Tempfli,† Mária Mátéfi-Tempfli,† Vlad Andrei Antohe,† Stéphane Fusil,‡ Karim Bouzehouane,‡ and Vincent Cros‡

Unité de Physico-Chimie et de Physique des Matériaux, Place Croix du Sud, 1, 1348-Louvain-la-Neuve, Belgium, and Unité Mixte de Physique CNRS/Thales and Université Paris Sud XI, Route Départementale 128, F-91767 Palaiseau Cedex, France

Received February 2, 2007; Revised Manuscript Received May 30, 2007

ABSTRACT

We have developed a new reliable method combining template synthesis and nanolithography-based contacting technique to elaborate current perpendicular-to-plane giant magnetoresistance spin valve nanowires, which are very promising for the exploration of electrical spin transfer phenomena. The method allows the electrical connection of one single nanowire in a large assembly of wires embedded in anodic porous alumina supported on Si substrate with diameters and periodicities to be controllable to a large extent. Both magnetic excitations and switching phenomena driven by a spin-polarized current were clearly demonstrated in our electrodeposited NiFe/Cu/ NiFe trilayer nanowires. This novel approach promises to be of strong interest for subsequent fabrication of phase-locked arrays of spin transfer nano-oscillators with increased output power for microwave applications.

There is currently great interest in studying effects related to spin transfer torque (STT) from a spin-polarized current in a nanosize ferromagnet. The potential applications are very promising, for example as a new way to write the information in nonvolatile memory.[1−5] High-frequency telecommunications constitute another field of applications of STT devices associated with the microwave emission induced by spin transfer.[6,7] The standard STT devices are either point contacts or nanopillars prepared by electron-beam lithography to achieve the high current density required to induce magnetic excitations or even magnetization reversal in multilayer spin valves.

In this work, we have been investigating a new method based on template synthesis for preparing magnetic nanowires appropriate for the study of spin transfer phenomena. We report on experimental results obtained in electrodeposited Py/Cu/Py (Py = $Ni_{80}Fe_{20}$) trilayer nanowires.

The template method is a general approach for preparing a variety of nanowires and nanostructures. This method entails synthesis using electrochemical techniques of a desired material within the cylindrical pores of a porous material. The diameters are often monodisperse and can be controlled routinely in the nm range. The template allows for unidirectional growth, making it easy to vary the composition of the nanowire in the axial direction. As a result, a nanowire of the desired material is obtained within each pore.

Electrodeposition into the pores of track-etched polymer and anodic aluminum oxide templates has proven to be reliable for the synthesis of a variety of magnetic nanowires and multilayers.[8−11] Filled membranes of these types have been used for the investigation of many original transport and magnetic properties such as current perpendicular to the planes giant magnetoresistance (CPP-GMR), field-induced magnetization reversal in single nanowires, domain wall magnetoresistance, quantized spin transport in nanoconstrictions, tunable magnetic anisotropy, and other phenomena due to dimensions comparable or smaller than scaling lengths in magnetism and spin-polarized transport.[12−14] While the template synthesis usually leads to the formation of large area nanowire arrays, spin transfer experiments require one to connect electrically a single nanowire and to inject a sufficiently high current density perpendicular to the plane of a GMR spin valve device. Though the CPP geometry requirement is naturally complied in the nanowire system, to address electrically one single nanowire is a more complicated challenge.

Different experimental approaches have been developed to establish an electrical contact on a single nanowire. A first approach is based on the use of optical or e-beam lithography technique to design specific electrodes to connect a single nanowire.[15−17] The process requires several steps

* Corresponding author. E-mail: piraux@pcpm.ucl.ac.be.
† Unité de Physico-Chimie et de Physique des Matériaux.
‡ Unité Mixte de Physique CNRS/Thales and Université Paris Sud XI.

10.1021/nl070263s CCC: $37.00
Published on Web 08/23/2007

prior to the lithography process that must be carefully optimized. It includes the dissolution of the membrane, the dispersion of an appropriate density of wires on a substrate, and the cleaning of the wires to remove all residues from the surface. The advantage of the lithography technique is that four-point electrical measurements can be performed on an isolated nanowire. Furthermore, segments as small as 500 nm can be probed.[15] However, the extremely high surface-to-volume ratio of the nanowires make them more sensitive to oxidation once removed from the template. Therefore, it is often difficult to prevent the nanowire from burning out by static discharge due to large resistance electrical contacts between the nanowires and the fingerlike electrodes (mainly caused by oxidation and imperfect cleaning of the nanowires). These problems preclude the study of spin transfer effects because large current densities are required (typically 10^7 A/cm^2).

Another approach has been developed with nanowires embedded in polymer membranes with relatively low pore density (typically less than 10^9 pores/cm^2). In this case, the wires can be easily top-contacted for electrical measurements using a self-contacting technique.[18,19] Using this procedure, a single nanowire is contacted reliably during the growth process and electrical contacts are therefore established on the two extremities of a 6−25 μm long nanowire (fixed by the thickness of the membrane). In contrast, the pore density is much higher in anodic porous alumina (up to 10^{11} pores/cm^2) making it difficult to contact a single wire by this method. Considering spin transfer studies, a clear drawback of this approach is the large aspect ratio of the contacted nanowire (typically more than 100), which is basically composed of a short three layer spin valve segment at the middle of a nonmagnetic nanowire. This leads to a strong additional resistance to the GMR spin valve device.[20] Therefore, the GMR signal is small, and strong heating problems occur due to Joule effect at high direct currents.

Recently, we have proposed a new reliable method[21] that allows the electrical connection of one single nanowire in a large assembly of wires embedded in a high pore density template (such as anodic porous alumina) supported on Si substrate. The use of supported alumina templates prevents one from breaking the fragile template during handling and/or nanocontact fabrication process.

The fabrication process begins with the anodization of ~0.8 μm thick Al layer sputtered onto the Ti/Au/Nb/Si substrate. The nanopores in the template are formed by complete anodic oxidation of the Al layer, performed in 0.3 M oxalic acid solution at 2 °C under a constant voltage of 60 V. At the end of the anodization process, residual alumina was eliminated completely from the bottom of all the nanopores by acid etching. The Au layer at the bottom of the pores serves as a working electrode for subsequent electrodeposition. The final thickness of the alumina template was about 1.1 μm, and the pore density was close to 5×10^9 cm^{-2}. The pore diameter was about 85 nm, and the interpore distance was 150 nm. Electrodeposition into the pores was carried out in a conventional three electrode cell with a platinum counter electrode and a Ag/AgCl reference

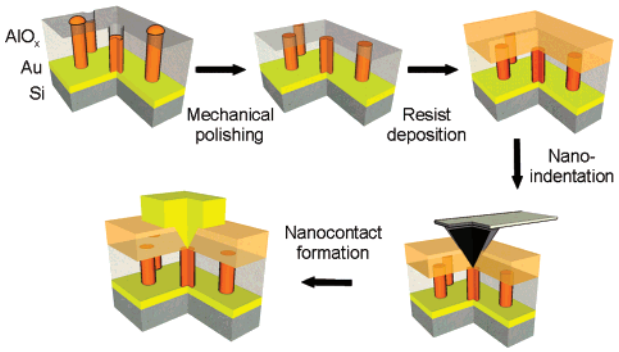

Figure 1. Schematic illustration of the single wire contacting process on an array of nanowires electrodeposited in supported nanoporous alumina template.

electrode. We used a single sulfate bath containing Ni, Fe, and Cu ions with the copper kept in dilute concentration.[22] We first deposit a 50 nm thick Cu layer at the bottom of the pores. Then, a trilayer structure Py(30 nm)/Cu(10 nm)/Py(6 nm) was electrodeposited by switching between the deposition potentials of the two constituents (respectively −0.5 and −1 V for Cu and Py deposition). To enhance the GMR signal, a same trilayer was subsequently deposited and separated from the former by a 100 nm thick Cu spacer layer. Finally, the pores were filled with Cu and the deposition process was stopped as soon as the first nanowires emerged at the surface.

Figure 1 illustrates the fabrication process used to create a nanocontact onto a single wire embedded in a thin alumina template. Prior to the nanolithography step, the template was thinned down to ≈100−200 nm by mechanical polishing with a resolution of a few tens of nm using colloidal silica (syton) in such a way that a large proportion of the nanowires end at the template surface. The lengths of the electrodeposited nanowires are thus almost uniform and equal to the thickness of the template.

Electrical nanocontacts on single wires are fabricated by indentation of an ultrathin insulating photoresist layer deposited on the top face of the thin porous alumina layer. A modified atomic force microscope designed for local resistance measurement is used as a nanoindenter, allowing an easy access point onto individual nanowires at the surface of the template. The indented holes are subsequently filled by metal to establish contacts on single nanowires. The interpore distance (150 nm) is significantly larger than the size of the hole (≈50 nm), and thus the probability to connect a single wire is very high. The area of each alumina template is less than 1 cm^2 on which are fabricated about 12 nanocontacts. More details about this nanofabrication process can be found in ref 21.

All transport measurements reported in this work were obtained at room temperature. The differential resistance dV/dI was measured using the lock-in technique with a 100 μA modulation current at f = 10 kHz added to a direct bias current. Current densities as large as 10^9 A/cm^2 were successfully injected on a single nanowire without deterioration. We define positive current such that the electrons flow

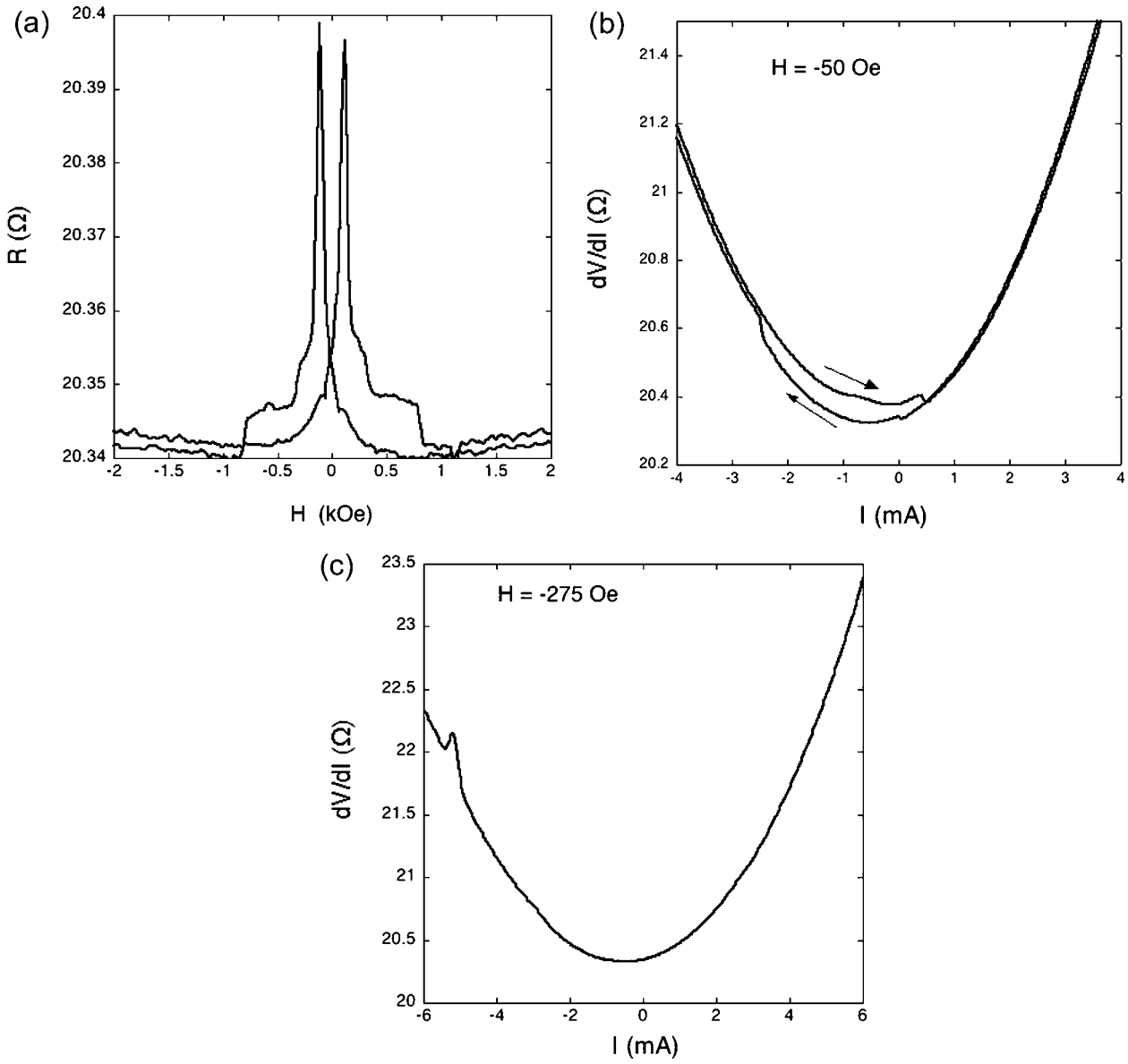

Figure 2. (a) GMR curve of Py(30 nm)/Cu(10 nm)/Py(6 nm) spin valve nanowire ($\phi = 85$ nm) with the magnetic field in the plane of the layer. (b) Differential resistance as a function of bias direct current at $H = -50$ Oe. Arrows mark the scan direction. (c) Differential resistance as a function of bias direct current at $H = -275$ Oe.

from the thick Py layer to the thin one. The magnetic field was applied perpendicular to the wire axis, that is, in the plane of the Py layers.

In Figure 2a, we show the magnetoresistance (MR) curve obtained on a Py/Cu/Py nanowire at zero direct current. The MR curve is symmetrically hysteretic with the magnetic field. The resistance of the wire gradually increases to the higher value with decreasing magnetic field from the positive saturation field. The antiparallel (AP) state is reached after passing the zero field. The observed behavior is typical of an almost uncoupled spin valve. The narrow plateau corresponding to the AP state results from the different coercive fields of the two Py layers. However, it is noted that the MR curve is not ideally square, as usually observed for electrodeposited GMR systems.[6] The MR ratio of 0.3% was obtained, and the difference in resistance between the AP and the parallel (P) states is around 60 mΩ.

In Figure 2b, we show the variation of the differential resistance dV/dI versus injected direct current at small field, that is, $H = -50$ Oe. Starting from the P state at zero current, the injected current is first decreased toward negative values. We first observed a sharp increase of the resistance at -2.5 mA due to the magnetization switching of the thin Py layer. The curve is hysteretic because the system remains in this high resistance state until the current is swept to a positive value. At a critical positive current of about + 0.4 mA, the resistance flips back to the P state level. The system remains in this low resistance state at higher positive current. In our convention, the electrons are flowing from the thick to the thin Py layer for positive current. The gradual increase in resistance with increasing bias current is due to the Joule effect.

The corresponding changes in the differential resistance estimated from Figure 2b are about 60−70 mΩ for both

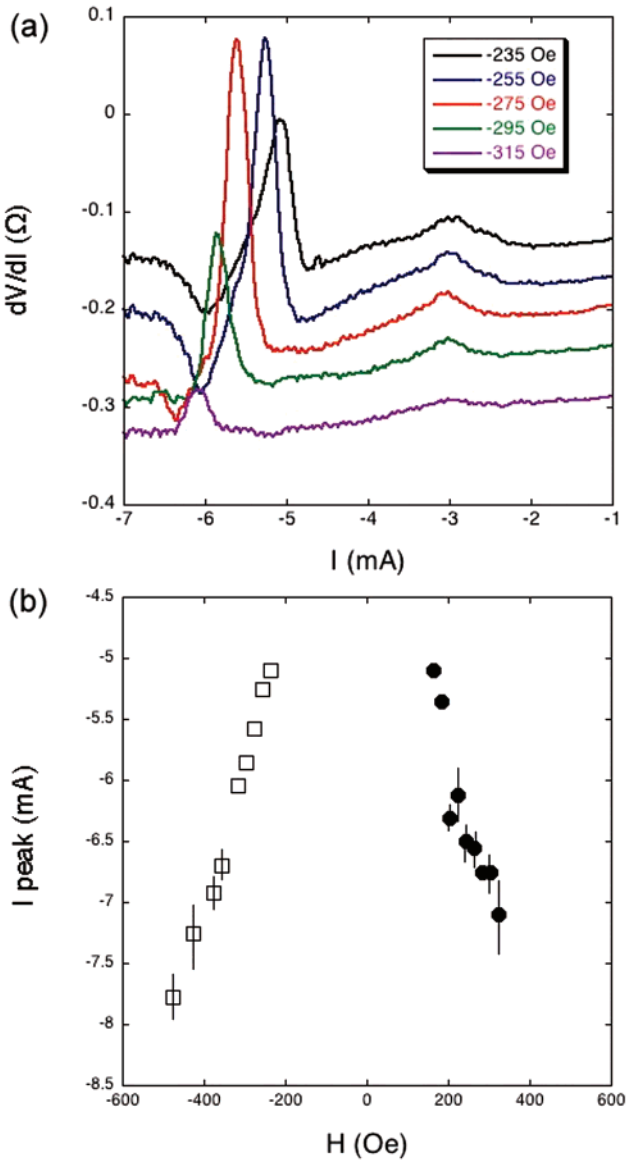

Figure 3. (a) Set of differential resistance curves for various magnetic fields (same sample as in Figure 2). The curves were obtained after subtraction of the measured differential resistance vs I by the monotonic dV/dI curve measured at −2000 Oe. The curves are offset for clarity. (b) I−H diagram for reversible switching peaks.

positive and negative switching, which corresponds to the change in resistance shown in the MR curve (Figure 2a). The critical current densities are estimated to be -4.4×10^7 A/cm^2 for the P to AP transition and 7×10^6 A/cm^2 for the AP to P transition. Therefore, the experimental hysteretic curve is attributed to spin transfer-induced magnetization reversal, usually observed at zero or low applied magnetic field.[4,5]

Under larger external magnetic field (typically larger than the coercive field of the thin Py layer), the abrupt jumps in the variation of the differential resistance with the injected direct current are replaced by reversible peaks (see in Figure 2c the dV/dI curve recorded at $H = -275$ Oe). As shown in Figure 3a, the position of the reversible peaks moves to higher current with increasing field. The curves in Figure 3a were obtained after subtraction of the dV/dI curves recorded at various magnetic fields from the curve measured at high field (−2000 Oe) in which no resistance steps were observed in the current range investigated, that is, up to 10 mA. However, at larger fields, we observe a strong decrease in peak amplitude and also an increase in the width of the peaks. For this particular sample, no reversible switching peaks can be detected at fields higher than −500 Oe. The magnetic field dependence of the critical currents for reversible switching is shown in Figure 3b for positive (respectively negative) fields after having applied negative (respectively positive) saturation fields. A slight field asymmetry is observed. It is found that the reversible switching peaks are generated by negative currents independently of the initial magnetic saturation direction. This feature is also a signature of the spin transfer torque, different from the effects of Oersted fields. The shift from irreversible to reversible action of the spin transfer torque has been associated in standard nanopillars to the onset of sustained precession of magnetization.[23,24]

We also emphasize that the average critical current densities (around 10^7 A/cm^2) measured on our electrodeposited nanowires are almost equal to those previously obtained on nanofabricated Py(30 nm)/Cu(10 nm)/Py(6 nm) nanopillars.[25,26] The same measurements were also performed on other nanowires of the same array, showing similar current-induced magnetization switching in the low-field range and reversible peaks of dV/dI at higher fields.

To summarize, we have described a new multistep process, which is very promising for the exploration of electrical spin transfer in magnetic nanostructures. The template approach for the fabrication of CPP spin valve nanowires is simple and flexible and provides an alternative to lithographic processes used for the fabrication of nanopillars and point contacts. Yet nanowires with ultralow diameters (a few nm) can be produced that are otherwise difficult to prepare using lithographic methods. Interestingly, the nanolithography-based contacting method allows one to connect separately individual nanowires at different locations on the same filled template and provides an easy way to perform single wire magneto-transport measurements. The electrodeposited nanowires can be specifically tailored to favor spin transfer torque effects. Both current-driven magnetic excitations and switching phenomena were clearly demonstrated in electrodeposited Py/Cu/Py trilayer nanowires.

Finally, it is well known that highly ordered arrays of magnetic nanowires can be fabricated using alumina templates with wire diameters and periodicities controllable to a large extent. Therefore, this novel approach promises ultimately to be of strong interest for the subsequent fabrication of coupled spin transfer nano-oscillators either through the emitted spin waves[27,28] or by an electrical coupling.[29]

Acknowledgment. This work was partly supported by the European Community's Sixth Framework Programme, Contrat NMP-CT-2004-505955 and the Interuniversity At-

traction Poles Program (P6/42), Belgian State, Belgian Science Policy.

References

(1) Slonczewski, J. *J. Magn. Magn. Mat.* **1996**, *159*, 1−7.
(2) Berger, L. *Phys. Rev. B* **1996**, *54*, 9353−9358.
(3) Tsoi, M.; Jansen, A. G. M.; Bass, J.; Chiang, W. C.; Seck, M.; Tsoi, V.; Wyder, P. *Phys. Rev. Lett.* **1998**, *80*, 4281−4284.
(4) Katine, J. A.; Albert, F. J.; Buhrman, R. A.; Myers, E. B.; Ralph, D. C. *Phys. Rev. Lett.* **2000**, *84*, 3149−3152.
(5) Grollier, J.; Cros, V.; Hamzić, A.; George, J. M.; Jaffrès, H.; Fert, A.; Faini, G.; Ben Youssef, J.; Legall, H. *Appl. Phys. Lett.* **2001**, *78*, 3663−3665.
(6) Kiselev, S.; Sankey, J. S.; Krivorotov, I. N.; Emley, N. C.; Schoelkopf, R. J.; Buhrman, R. A.; Ralph, D. C. *Nature* **2003**, *425*, 380−383.
(7) Rippard, W. H.; Pufall, M. R.; Kaka, S.; Russek, S. E.; Silva, T. J. *Phys. Rev. Lett.* **2004**, *92*, 027201.
(8) Arai, K. I.; Ishiyama, K.; Ohoka, Y.; Kang, H. W. *J. Magn. Soc. Jpn* **1989**, *13*, 789−794.
(9) Whitney, T. M.; Jiang, J. S.; Searson, P. C.; Chien, C. L. *Science* **1993**, *261*, 1316−1319.
(10) Piraux, L.; George, J. M.; Despres, J. F.; Leroy, C.; Ferain, E.; Legras, R.; Ounadjela, K.; Fert, A. *Appl. Phys. Lett.* **1994**, *65*, 2484−2486.
(11) Blondel, A.; Meier, J. P.; Doudin, B.; Ansermet, J. P. *Appl. Phys. Lett.* **1994**, *65*, 3019−3021.
(12) Fert, A.; Piraux, L. *J. Magn. Magn. Mater.* **1999**, *200*, 338−358.
(13) Ansermet, J. P. *J. Phys.: Condens. Matter* **1998**, *10*, 6027−6050.
(14) Piraux, L.; Encinas, A.; Vila, L.; Mátéfi-Tempfli, S.; Mátéfi-Tempfli, M.; Darques, M.; Elhoussine, F.; Michotte, S. *J. Nanosci. Nanotechnol.* **2005**, *5*, 372−389.
(15) Vila, L.; Piraux, L.; George, J. M.; Fert, A.; Faini, G. *Appl. Phys. Lett.* **2002**, *80*, 3805−3807.
(16) Toimil Molares, M. E.; Höhberger, E. M.; Schaeflein, C.; Blick, R. H.; Neumann, R.; Trautmann, C. *Appl. Phys. Lett.* **2003**, *82*, 2139−2141.
(17) Tanase, M.; Silevitch, D. M.; Chien, C. L.; Reich, D. H. *J. Appl. Phys.* **2003**, *93*, 7616−7618.
(18) Wegrowe, J. E.; Kelly, D.; Franck, A.; Gilbert, S. E.; Ansermet, J. P. *Phys. Rev. Lett.* **1999**, *82*, 3681−3684.
(19) Pignard, S.; Goglio, G.; Radulescu, A.; Piraux, L.; Duvail, J. L.; Dubois, S.; Declémy, A. *J. Appl. Phys.* **2000**, *87*, 824−829.
(20) Wegrowe, J. E.; Fabian, A.; Guittienne, P.; Hoffer, X.; Kelly, D.; Ansermet, J. P. *Appl. Phys. Lett.* **2002**, *80*, 3775−3777.
(21) Fusil, S.; Piraux, L.; Mátéfi-Tempfli, S.; Mátéfi-Tempfli, M.; Michotte, S.; Saul, C. K.; Pereira, L.; Bouzehouane, K.; Cros, V.; Deranlot, C.; George, J. M. *Nanotechnology* **2005**, *16*, 2936−2940.
(22) Dubois, S.; Marchal, C.; Beuken, J.-M.; Piraux, L.; Duvail, J.-L.; Fert, A.; George, J.-M.; Maurice, J.-L. *Appl. Phys. Lett.* **1997**, *70*, 396−398.
(23) Grollier, J.; Cros, V.; Jaffres, H.; Hamzic, A.; George, J. M.; Faini, G.; Ben Youssef, J.; Le Gall, H.; Fert, A. *Phys. Rev. B* **2003**, *67*, 174402 (1−8).
(24) Cros, V.; Boulle, O.; Grollier, J.; Hamzic, A.; Munoz, M.; Pereira, L. G.; Petroff, F. *C. R. Physique* **2005**, *6*, 956−965.
(25) Urazhdin, S.; Birge, N. O.; Pratt, W. P.; Bass, J. *Phys. Rev. Lett.* **2003**, *91*, 146803 (1−4).
(26) Kiselev, S.; Sankey, J. S.; Krivorotov, I. N.; Emley, N. C.; Garcia, A. G. F.; Buhrman, R. A.; Ralph, D. C. *Phys. Rev. B* **2005**, *72*, 064430 (1−10).
(27) Kaka, S.; Pufall, M. R.; Rippard, W. H.; Silva, T. J.; Russek, S. E.; Katine, J. A. *Nature* **2005**, *437*, 389−392.
(28) Mancoff, F. B.; Rizzo, N. D.; Engel, B. N.; Tehrani, S. *Nature* **2005**, *437*, 393−395.
(29) Grollier, J.; Cros, V.; Fert, A. *Phys. Rev. B* **2006**, *73*, 060409(R).

NL070263S